Injectable, Highly Flexible, and Thermosensitive Hydrogels Capable of Delivering Superoxide Dismutase

Zhenqing Li,[†,‡] Feng Wang,[†,‡] Sashwati Roy,[§] Chandan K. Sen,[§] and Jianjun Guan*[,‡]

Department of Materials Science and Engineering, The Ohio State University, Columbus, Ohio 43210, and Davis Heart and Lung Research Institute, The Ohio State University, Columbus, Ohio 43210

Received August 7, 2009; Revised Manuscript Received October 27, 2009

Injectable hydrogels are attractive for cell and drug delivery. In this work, we synthesized a family of injectable, biodegradable, fast gelling and thermosensitive hydrogels based on *N*-isopropylacrylamide (NIPAAm), acrylic acid (AAc), dimethyl-γ-butyrolactone acrylate (DBA), and 2-hydroxyethyl methacrylate-poly(trimethylene carbontate) (HEMAPTMC) macromer. Type I collagen was composited with the hydrogels to improve their biocompatibility. The hydrogel copolymer solutions were readily injectable at 4 °C. The solutions exhibited thermal transition temperatures ranging from 23.6 to 24.5 °C and were capable of gelation within 7 s at 37 °C to form highly flexible and soft hydrogels with moduli from 39 to 119 KPa and breaking strains >1000%, depending on the copolymer composition and collagen addition. After 2 weeks incubation in PBS, the hydrogels demonstrated weight losses ranging from 10−20%. The completely degraded hydrogels had thermal transition temperatures >40 °C and were soluble at body temperature. Superoxide dismutase (SOD) was encapsulated in the hydrogels for the purpose of capturing superoxide within the inflammatory tissue after being delivered in vivo. The hydrogels demonstrated a sustained release profile during a 21-day release period. The release kinetics was dependent on the SOD loading, collagen addition, hydrogel degradation and water content. The released SOD remained bioactive during the entire release period. To test in vitro if the loaded SOD could protect cells encapsulated within the hydrogel from attack by superoxide, human mesenchymal stem cells (MSC) were encapsulated in SOD-loaded hydrogels and cultured in medium containing superoxide generated by activated macrophages. It was found that SOD loading largely suppressed superoxide penetration into the hydrogel and cell membrane. Under normal culture conditions, SOD loading stimulated MSC growth. The SOD-loaded hydrogel exhibited significantly higher cell numbers than the non-SOD loaded hydrogel during a 7-day culture period. These results demonstrated that the developed hydrogels could be used as delivery vehicles for stem cell therapy and drug delivery.

1. Introduction

Injectable hydrogels are widely used in drug delivery and tissue engineering fields because of their injectability, good permeability, high water content, and tissue-like mechanical properties.[1] Various polymers, including natural polymers, like collagen,[2] gelatin,[3] chitosan,[4] and hyaluronic acid,[5] and synthetic polymers, such as poly(ethylene glycol), poly(vinyl alcohol),[6−8] and polylactide-*co*-poly(ethylene glycol)-*co*-polylactide (PLA-PEG-PLA),[9] have been used as injectable hydrogels. Of these, thermosensitive hydrogels are of particular interest as they are capable of gelation by a simple altering of temperature. There is no need for chemical/photo-cross-linking that may raise a cytotoxicity issue. In addition, thermosensitive hydrogels may be easily delivered in vivo using procedures such as minimum invasive surgery. Thermosensitive polymers based on PLA-PEG-PLA or poly(*N*-isopropylacylamide) (PNIPAAm) have been widely used.[10−13]

The major disadvantage of PNIPAAm hydrogels is their nondegradability, which greatly limits their application in tissue engineering. Various efforts have been undertaken to make biodegradable PNIPAAm hydrogels. These include copolymerization of PNIPAAm with degradable polymers[14] and cross-linking PNIPAAm copolymers with enzyme-sensitive peptides.[15] However, these methods usually yield cross-linked hydrogels that have limited injectability. Therefore, they can not be delivered using a convenient injection technique. To overcome this limitation, we previously generated a family of linear PNIPAAm-based copolymers that possess thermal transition temperatures lower than 37 °C before degradation and higher than 37 °C after degradation. This allows them to be injectable at temperatures lower than the transition temperature before degradation, and to be soluble at 37 °C after degradation.[10] The copolymers were synthesized from NIPAAm, acrylic acid, *N*-acryloxysuccinicimide, and hydroxyethyl methacylate-polylactide. Interestingly, the formed hydrogels were highly flexible at body temperature with a breaking strain >1000%. The disadvantage of these hydrogels is their relatively high degradation rate (weight loss >80% over 2 weeks) resulting from fast degrading polylactide segments. One of the purposes in this work was to develop hydrogels that have a slower degradation rate while retaining good mechanical properties.

One of the applications of these flexible and injectable hydrogels may be soft tissue cell therapy, as the cells can be easily mixed with the injectable hydrogel polymer solution. In addition, the highly flexible nature of the hydrogels enables them to respond to soft tissue motion. The mesenchymal stem cell (MSC), a multipotent stem cell, has been widely used for soft tissue cell therapy as it can differentiate into multiple cell lineages.[16−20] In addition, the MSC has been demonstrated to improve angiogenesis in vivo.[17] However, direct injection of MSC often yields an extremely low cell engraftment a few

* To whom correspondence should be addressed. Phone: 614-292-9743. E-mail: guan.21@osu.edu.
[†] These authors contributed equally to this work.
[‡] Department of Materials Science and Engineering.
[§] Davis Heart and Lung Research Institute.

10.1021/bm900900e CCC: $40.75
Published on Web 11/17/2009

weeks after transplantation. This is due to the lack of a protective environment for cells to avoid direct attack from immune response, and the lack of a matrix for cells to attach to, leading to apoptosis.[19,20] It is hypothesized that encapsulation of MSCs within the hydrogel would largely improve cell engraftment, because the hydrogel would not only protect the cell but also provide a matrix for cells to attach. However, hydrogels are inefficient at inhibiting low molecular weight cytotoxic species such as reactive oxygen species (ROS) from penetrating into hydrogels and damaging the encapsulated cells. ROS is believed to play an important role in cell death after tissue injury.[21−23] Superoxide dismutase, a nonscavenger enzyme capable of catalyzing the dismutation of superoxide into the less toxic hydrogen peroxide and molecular oxygen, has been widely used as an antioxidant for decreasing ROS content in injured tissues.[24−26] Superoxide dismutase (SOD) delivery often needs repeated administration to reach therapeutic effect due to its short half-life. Efforts have been made to encapsulate SOD into microspheres, scaffolds, and hydrogels.[27,28] The major disadvantages of current encapsulation systems lie in their low SOD encapsulation efficiency and loss of bioactivity in a short time.[26,29−34] To address these issues, SOD mimetics have been encapsulated in scaffolds and hydrogels. However, their release rates are high due to a relatively low molecular weight. Thus, they are unable to provide long-term therapeutic effect.[35]

The objectives of this work were (1) to synthesize slow degrading, highly flexible, and injectable hydrogels, and (2) to explore the feasibility of synthesized hydrogels for sustained (>1 week) delivery of bioactive SOD so as to protect encapsulated cells from attack by superoxide, leading to improve cell survival after implantation. To reach these goals, we developed a new family of hydrogels that have slow degradation rates. These hydrogels were shown to be capable of releasing bioactive SOD during the 3-week release period. In addition, SOD encapsulation protected MSCs from attack by ROS and stimulated MSC growth.

2. Materials and Methods

2.1. Materials. All materials and reagents were purchased from Sigma unless otherwise stated. *N*-Isopropylacrylamide (NIPAAm) was purified by recrystallization with ethyl acetate and hexane. 2-Hydroxyethyl methacylate (HEMA) and acrylic acid (AAc) were purified by removing the inhibitor through the inhibitor removal column. Trimethylene carbonate (TMC, Boehringer Ingelheim) was vacuum-dried before use. Acryloyl chloride, pantolactone, stannous octate, tetrahydrofuran, dioxane, ethyl acetate, and hexane were purchased from Acros and used as received. SOD from bovine erythrocyte was purchased from Sigma-Aldrich.

2.2. Synthesis of Hydrogel Copolymers. The macromer HEMAPTMC was synthesized by reacting HEMA with TMC (molar ratio 1:2) under 110 °C for 1 h using stannous octate as a catalyst. After reaction, the mixture was dissolved in THF and precipitated in cold deionized water. The precipitate was redissolved in ethyl acetate and dried by magnesium sulfate. The ethyl acetate was then removed at reduced pressure. The resulting macromer had a HEMA/TMC ratio of 1:2.1, as calculated from the ^{1}H NMR ($CDCl_3$) integral area of the protons from HEMA unit ($C\underline{H}_2$, 6.02 and 5.68 ppm, respectively; $C\underline{H}_3-$, 1.95 ppm; $-OC\underline{H}_2C\underline{H}_2O-$, 4.33 ppm) and TMC unit ($-OC\underline{H}_2CH_2C\underline{H}_2O-$, 4.11 ppm; $-OCH_2C\underline{H}_2CH_2O-$, 1.91 ppm).

Dimethyl-γ-butyrolactone acrylate (DBA) was synthesized by acylation of pantolactone. Briefly, acryloyl chloride (0.231 mol) was added dropwise into a single-necked 1000 mL flask containing dimethyl-γ-butryolactone (0.231 mol), methylene chloride, and triethylamine at 0 °C. The reaction was conducted for 3 h. The mixture was then filtered. The solution was washed with DI water three times and dried with magnesium sulfate. The solvent was evaporated under reduced pressure. The structure of the DBA was confirmed by ^{1}H NMR ($CDCl_3$): 6.25 and 6.00 ($C\underline{H}_2$), 6.53 ($=C\underline{H}-$), 5.45 and 5.29 ($-C\underline{H}-$), 4.05 ($-COOC\underline{H}_2-$), 1.15, 1.25 ppm ($-C\underline{H}_3$).

The hydrogel copolymers were synthesized from NIPAAm, AAc, dimethyl-γ-butyrolactone acrylate (DBA), and hydroxyethyl methacrylate-poly(trimethylene carbonate) (HEMAPTMC, Figure 1) by free radical polymerization using benzoyl peroxide as an initiator.[10,36] Stoichiometrical amounts of NIPAAm, AAc, DBA, and HEMAPTMC dissolved in dioxane were added into a 500 mL three-necked flask equipped with a nitrogen inlet and outlet. The solution was bubbled with nitrogen for 15 min before the flask was immersed into a 70 °C oil bath. The degassed benzoyl peroxide was then injected into the flask. After 24 h of reaction, the solution was cooled to room temperature. The polymer was precipitated with hexane and purified twice by dissolving it in THF and precipitating it from ethyl ether. The polymers were abbreviated according to the feed ratio of NIPAAm, DBA, AAc, and HEMAPTMC (Table 1).

2.3. Preparation of Hydrogel and Collagen Biocomposites. The hydrogel and collagen biocomposites were prepared by mixing a hydrogel copolymer solution with type I collagen. The copolymer with feed ratio of 90/4/2/4 was dissolved in phosphate buffered saline (PBS, pH = 7.4) at 4 °C to form a 20 wt % solution. The defined amount of type I collagen (Kensey Nash Inc.) in PBS solution (6 wt %) was added into the copolymer solution. After a thorough mixing, the mixture was set at 4 °C overnight.

2.4. Polymer Characterization. Structure of the hydrogel copolymers was characterized by ^{1}H NMR and FT-IR. ^{1}H NMR spectra were recorded by a 400 MHz spectrometer (Bruker) using $CDCl_3$ (Sigma) as a solvent. FT-IR spectra were conducted in a FT-IR spectrometer (Thermo Fisher, Nicolet 8700). For molecular weight characterization, 200 μL of copolymer in THF (0.1 wt %) was injected into a gel permeation chromatography (GPC, Waters). Number average, weight average molecular weights, and polydispersity (PDI) were obtained. Polystyrene was used as a standard.

Glass transition temperatures (T_gs) of the hydrogel copolymers were measured by differentiated scanning calorimetry (DSC, TA Instrument) over the temperature range of −100 to 200 °C with a heating rate of 20 °C/min. The T_g of hydrogel/collagen biocomposite was measured after lyophilization of the aqueous mixture. To determine thermal transition temperatures of the hydrogel copolymer and copolymer/collagen solutions, a temperature range of 0 to 90 °C, and a heating rate of 10 °C/min were used. The temperature at the position of the maximum endothermal peak in the DSC curve was considered as the thermal transition temperature. This transition is a result of conformation change of the PNIPAAM macromolecules (coil to globule). The thermal transition temperature of the completely degraded hydrogel copolymer solution was also measured. To obtain the completely degraded hydrogel copolymer, the copolymer (90/4/2/4) was immersed into 1 M sodium hydroxide solution for hydrolysis at 60 °C. The pH of the solution was maintained at 14. The solution was then cooled to room temperature and neutralized with 1 M hydrochloride solution. The formed clear solution was then extracted with methylene chloride and followed by evaporation under reduced pressure. The completely degraded copolymer was then dissolved in PBS for the thermal transition temperature measurement. Molecular weight of the completely degraded copolymer was determined by GPC using THF as a solvent.

Gelation time of the hydrogel copolymer solutions was measured in a microscope (IX71, Olympus) equipped with a temperature control system (Weather Station, Precisioncontrol Inc.) and a video recorder (DP70, Olympus). The system was prewarmed to 37 °C before testing. A total of 20 μL of the hydrogel copolymer solution was dropped on a prewarmed glass slide. The turbidity was recorded. The light intensity was processed by NIH Image J software. Linear fit was used to interpolate the intensity drop region and then extrapolated to the initial and final intensity plateau. The time interval between the two

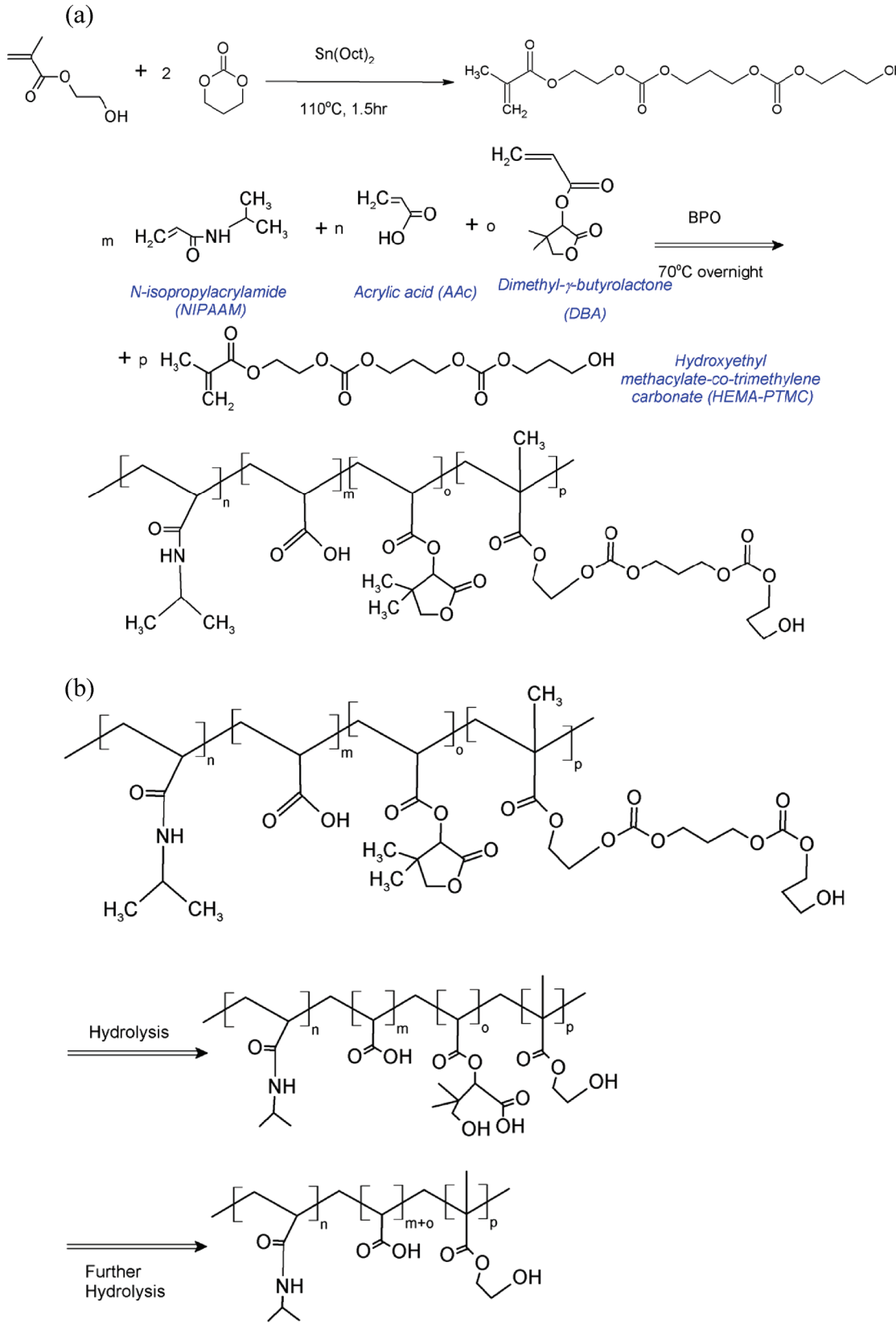

Figure 1. Synthesis scheme of macromer and hydrogel (a) and the mechanism of hydrolysis (b).

intersections was considered as the gelation time. Injectability of the hydrogel copolymer solutions was tested by their ability to be injected through a 26 gauge needle. This was based on the consideration that animal injections usually employ needles as small as 26 gauge. The hydrogel copolymer solution (4 °C) was filled into a 1 mL syringe equipped with a 26 gauge needle. The syringe was then cooled in a 4 °C refrigerator before being manually injected.

To test hydrogel water content, hydrogel copolymer solution (20 wt %) was injected into a 96-well plate (200 μL/well). The covered plate was placed into a 37 °C water bath for 5 h. The hydrogel pellets were

Table 1. Copolymer Composition and Molecular Weight Characterization

copolymer	feed ratio	composition[a]	M_n	PDI	M_n after degradation
90/2/4/4	90/2/4/4	90/1.5/4.3/4.2	15600	2.5	
90/4/2/4	90/4/2/4	90/3.9/1.9/4.2	13700	2.1	10100

[a] Calculated by ^{1}H NMR.

taken out and gently wiped with tissue paper to remove surface water. The wet weight of hydrogel was measured (w_1). The hydrogel was then lyophilized for 2 days and the dry weight was taken (w_2). The water content was calculated as

$$\text{water content} = (w_1 - w_2)/w_1 \times 100\%$$

2.5. Hydrogel Mechanical Properties. Tensile mechanical properties of the hydrogels were characterized at 37 °C using the method described previously.[10] Before testing, 2 μL of 20 wt % hydrogel copolymer or copolymer/collagen composite solution in a 20 mL vial were placed in a 37 °C water bath to form a hydrogel. The hydrogel was maintained in the water bath for 5 h before being removed from the vial and cut into a rectangular shape with a width of 3 mm and a length of 25 mm. To ensure that the sample loading process did not cause sample defects due to thermosensitive nature of the hydrogel, the grips were preheated at 37 °C before the samples were loaded. The testing was conducted in a 37 °C water bath using an Instron load frame (model 1322). A cross-head speed of 50 mm/min was used. At least five samples were evaluated for each condition.

2.6. Hydrogel Degradation. Hydrogel degradation at 37 °C in PBS (pH = 7.4) was measured over a 2 week period. The fixed volume (~250 μL) of 20 wt % hydrogel copolymer solution was added into a 2 mL microcentrifuge tube. The tube was placed in a 37 °C water bath for gelation and the formed gel was maintained in the water bath for 5 h. The supernatant was then taken out and an equal volume of prewarmed PBS was added. The degradation was conducted at 37 °C. The samples were taken at defined intervals, gently wiped with tissue paper, and weighed (w_2). The hydrogel was then vacuum-dried at 60 °C for 2 days before being weighed (w_3). The water content of the degrading hydrogel was calculated as described above. The weight remaining was calculated as

$$\text{weight remaining}(\%) = w_3/w_1 \times 100\%$$

where w_1 is the sample weight before degradation. This is equal to the calculated weight from the defined volume and concentration minus dry mass of the supernatant. At least five samples were evaluated for each hydrogel type.

2.7. SOD Encapsulation and Release. To load SOD in the hydrogel, 1 mL of hydrogel copolymer solution (20 wt %) was thoroughly mixed with 100 μL of SOD solution (in PBS, concentration 2 or 4 mg/mL) at 4 °C overnight. A total of 200 μL of the mixed solution was then transferred into a 2 mL Eppendorf tube. The tube was kept in a 37 °C water bath for 30 min for gelation. The supernatant was removed. A total of 200 μL of PBS was then added into the tube. The release was conducted at 37 °C in a water bath. At predefined time points (4 and 8 h, and 1, 3, 7, 10, 14, and 21 d), the supernatant was collected and replaced with an equal volume of PBS. The collected SOD solution was placed in a Biomat3 UV/vis spectrometer (Thermo Scientific) to measure UV absorbance at 250 nm. SOD content was calculated according to a SOD standard curve. Bioactivity of the released SOD was measured spectrophotometrically by a SOD Assay Kit-WST (Fluka) in accordance with the manufacturer's instructions.

2.8. Mesenchymal Stem Cell Encapsulation. Human bone marrow derived mesenchymal stem cells (MSCs, Lonza) were plated in Dulbecco's modified Eagle's minimum essential medium (DMEM) and supplemented with 10 wt % fetal bovine serum (Atlanta Biologics), 2% L-glutamine (Gibco), and 1% penicillin/streptomycin (Lonza). The cells between passage 12 and 14 were used. These cells have been shown to be multipotent as confirmed by RT-PCR data (see Supporting Information) and in previous reports.[37]

Hydrogel and hydrogel/collagen biocomposite encapsulated with or without 4 mg/mL SOD were prepared as described above. MSCs labeled with live cell marker CellTracker Green CMFDA (5-chloromethylfluorescein diacetate, concentration 10 μM) were suspended in PBS to obtain a cell suspension with a density of 40 million/mL. A total of 0.25 mL of cell suspension was added into 1 mL of the hydrogel copolymer or copolymer/collagen solution. The mixture was thoroughly mixed at 4 °C before being transferred into 37 °C water bath for gelation. The supernatant was then removed and replaced with culture medium (PBS supplemented with 10% FBS, 2% L-glutamine, and 1% penicillin/streptomycin). The medium was changed every 3 days. After 1 and 7 days of culture, samples were taken out and digested with papain solution (0.125 mg/mL papain in 100 mM sodium phosphate, 10 mM EDTA buffer, 100 mM L-cystein, pH = 6.5) at 60 °C until all the hydrogel was dissolved. The DNA content was quantified with PicoGreen dsDNA assay (Invitrogen). To image the cells in the hydrogel, samples were cut into 100 μm thick sections and observed directly under fluorescent microscopy (Olympus IX-71, equipped with a DP70CCD camera).

2.9. Mesenchymal Stem Cell Culture in the Presence of Superoxide. To test if SOD loading would inhibit superoxide penetration into the hydrogel and improve survival of encapsulated cells, the MSC-encapsulated hydrogel/collagen biocomposite was cultured in the presence of superoxide. Before encapsulation, MSCs were labeled with a cell-permeant indicator for reactive oxygen species, H_2DCFDA (2′,7′-dichlorofluorescin diacetate, Invitrogen), which is nonfluorescent until the acetate groups are removed by intracellular esterases and oxidation occurs within the cell. The labeled MSCs (40 million/mL) were encapsulated into the hydrogel biocomposite to obtain a final density of 10 million/mL. After gelation in the 37 °C water bath, the formed hydrogel was punched into 6 mm diameter disks, which were then placed into a 6-well plate. A total of 1 mL of culture medium was added to each well. Superoxide was generated by adding 200 ng/mL phorbol-12-myristate 13-acetate (PMA) into the macrophage-populated (1×10^6 per well) transwell (pore size 0.4 μm) that contained 1 mL of macrophage culture medium (RPMI 1640 supplemented with 10% fetal bovine serum and 1% penicillin/streptomycin). The hydrogel samples were taken out after 4 and 20 h of incubation, and the fluorescent intensity was recorded by a fluorescent microplate reader (Tecan Genios Pro, Tecan). The hydrogels that did not load with SOD but seeded with H_2DCFDA stained MSC and cultured in the presence of activated macrophage, and that loaded with SOD and seeded with H_2DCFDA stained MSC but cultured without macrophage, were used as controls.

2.10. Statistical Analysis..[38] Each experiment was conducted at least in triplicate ($n \geq 3$). One-way ANOVA was used for all the experiments unless otherwise stated. Two-way ANOVA was performed for cell growth within the hydrogels. $p < 0.05$ was considered to be significantly different.

3. Results

3.1. Hydrogel Copolymer Structure Characterization. Structures of the synthesized copolymers were confirmed by FT-IR and ^{1}H NMR (Figures 2 and 3). FT-IR spectrum (Figure 2) shows that the copolymer had characteristic absorptions of the isopropyl group (1460, 1380, and 1360 cm^{-1}), amide group (1530 and 1640 cm^{-1}), carboxylic group (1 713 cm^{-1}), and carbonyl group of HEMAPTMC units (1750 cm^{-1}) and DBA units (1780 cm^{-1}), respectively. In ^{1}H NMR spectrum (Figure

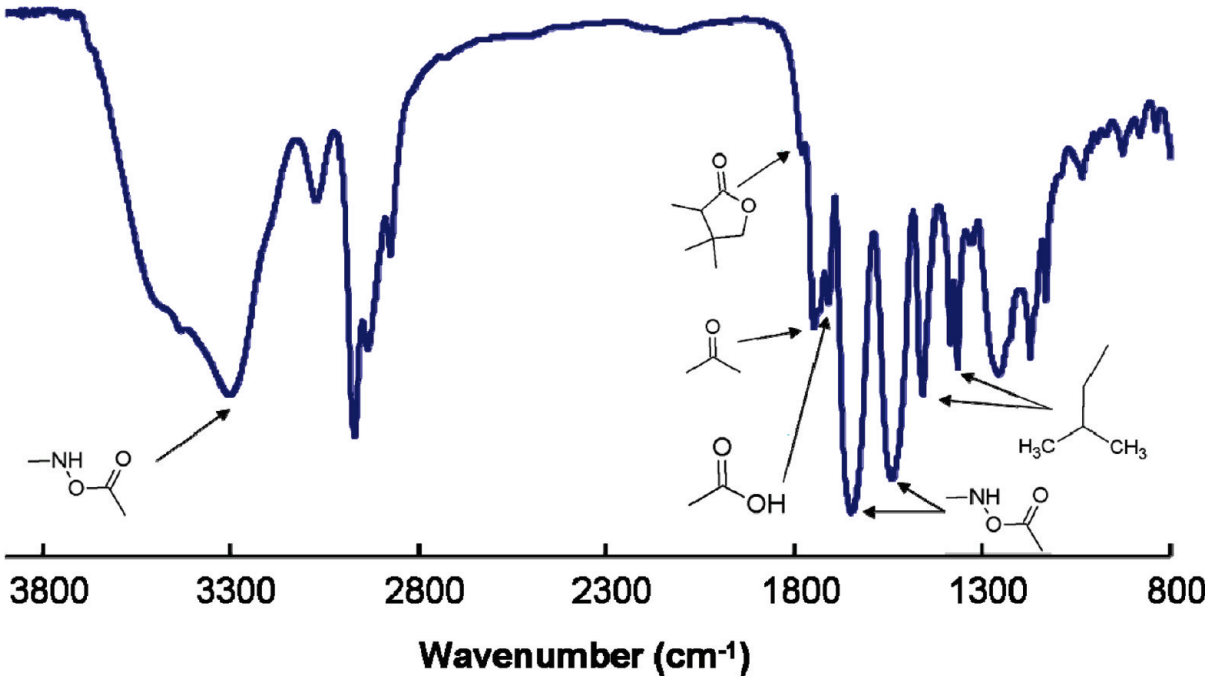

Figure 2. FT-IR spectrum of synthesized hydrogel.

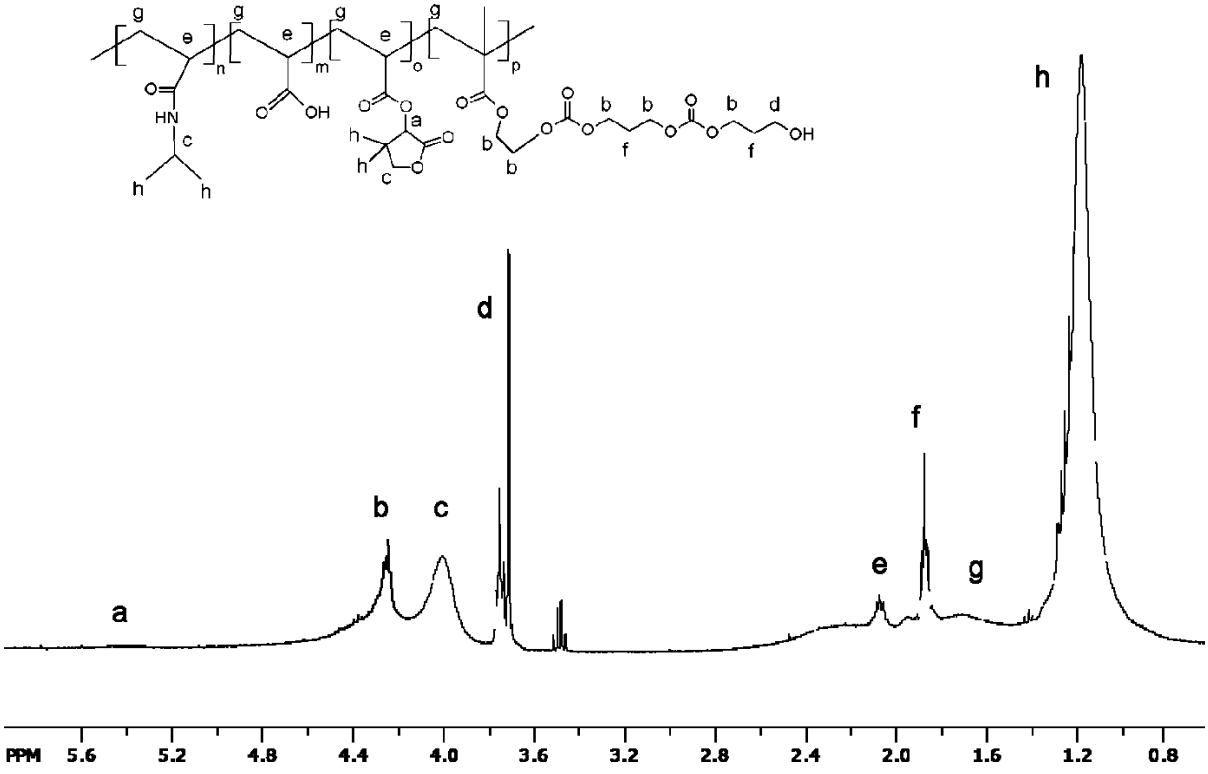

Figure 3. ^{1}H NMR spectrum of synthesized hydrogel.

3), the hydrogel copolymers demonstrated characteristic proton peaks of HEMAPTMC units (b, d, f, and g), DBA units (a, c, e, and g), AAc units (e and g), and NIPAAm units (c, e, and g). Composition of the hydrogel copolymer was calculated from the integration area ratio of the characteristic proton peaks from each monomer unit. It was found that all of the hydrogels had composition consistent with the feed ratio. GPC results showed that number-average molecular weights were greater than 13700 Da (Table 1).

3.2. Hydrogel Copolymer Thermal Properties. Hydrogel copolymer thermal properties in dry and wet states were characterized by DSC (Table 2). The dry copolymers exhibited glass transition temperatures (T_gs) between 126.3−132.1 °C, depending on the AAc content and collagen addition. The hydrogel copolymer with higher AAc content demonstrated a higher T_g. Incorporation of collagen increased T_g from 129.7 to 132.1 °C.

Thermal transition temperatures of the hydrogel copolymer solutions before and after degradation are presented in Table 2. Before degradation, all of the copolymer solutions possessed thermal transition temperatures ranging from 23.6 to 24.8 °C, depending on the AAc content and collagen addition. Higher

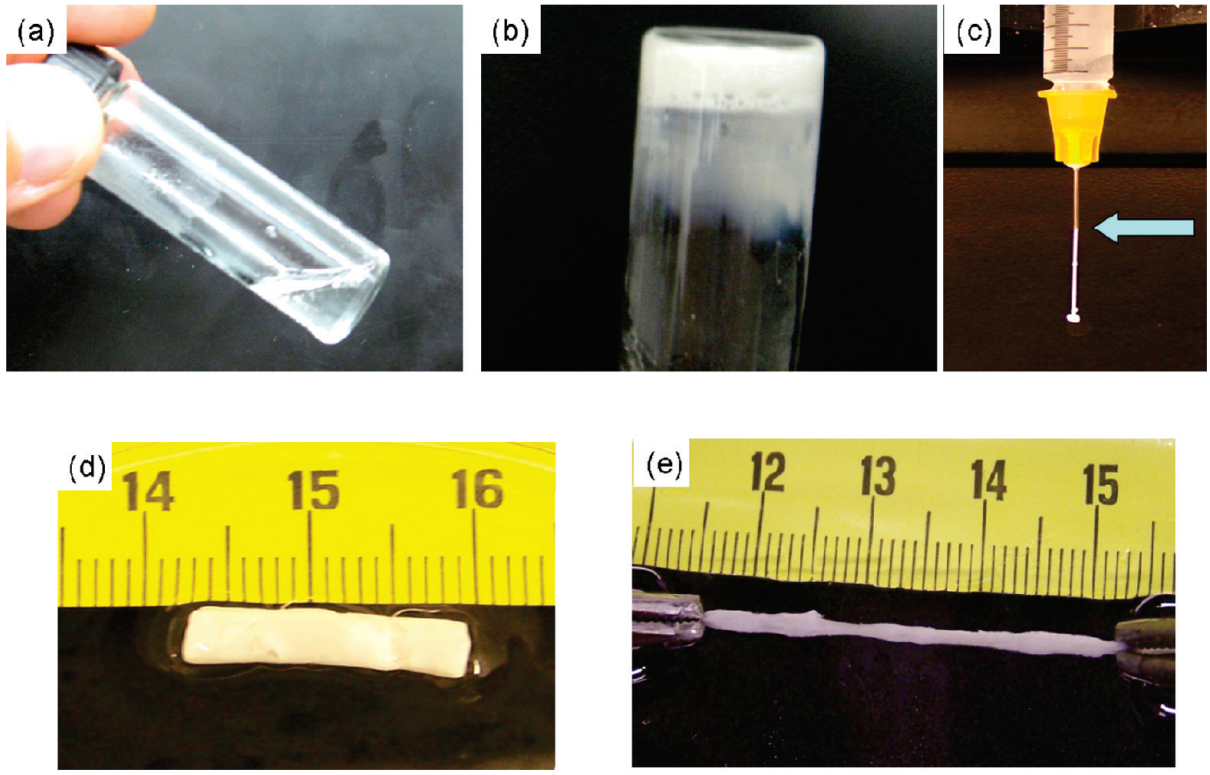

Figure 4. Macroscopic images of hydrogel. The copolymer solution is flowable at 4 °C (a) and forms gel after gelation at 37 °C (b). The copolymer solution can be injected through a 26 gauge needle (c). At 37 °C, the formed gel is flexible and can be stretched: (d) before stretching; (e) after stretching.

Table 2. Thermal Properties, Gelation Time, Injectability, and Water Content of the Hydrogels

hydrogel	T_g (°C)	thermal transition temperature before degradation (°C)	thermal transition temperature after degradation (°C)	gelation time (s)	injectability	water content (%)
90/2/4/4	126.3	23.6	44.2	7	+	49 ± 4
90/4/2/4	129.7	24.8	47.4	6	+	83 ± 8
90/4/2/4 + collagen	132.1	26.4		5	+	124 ± 18

Table 3. Hydrogel Mechanical Properties

hydrogel	breaking strain (%)	tensile stress (KPa)	initial modulus (KPa)
90/2/4/4	>1000	14.7 ± 1.6	43.3 ± 18.6
90/4/2/4	>1000	19.3 ± 2.7	55.9 ± 9.1
90/4/2/4 + collagen	>1000	29.0 ± 5.1	119.3 ± 14.2

AAc content showed a higher transition temperature, while collagen addition increased the thermal transition temperature. To measure the thermal transition temperature of the completely degraded copolymer solution, the hydrogels were immersed in a NaOH solution to completely hydrolyze the DBA side group and PTMC side chain. The resulting copolymer theoretically exhibits the same structure as those completely degraded in PBS (Figure 1). The hydrolyzed copolymer possessed a thermal transition temperature greater than 44.2 °C, demonstrating that the completely degraded copolymer was soluble at body temperature.

3.3. Hydrogel Copolymer Solution Injectability, Gelation Time, and Water Content. The hydrogel copolymer solutions were flowable at temperatures below thermal transition temperatures (Figure 4a). Injectability of the copolymer solution was tested by injecting a 20 wt %, 4 °C solution through a 26 gauge needle (Figure 4c). It was found that all the hydrogel copolymer solutions could be readily injected through the needle, indicating that these hydrogel copolymers may be used for soft tissue injection where needles as small as 26 gauge are often used. Once placed at 37 °C, all the hydrogel copolymer solutions were able to quickly form solid hydrogels (Figure 4b). The time needed for a 20 μL, 4 °C hydrogel solution to form a solid hydrogel at 37 °C was defined as the gelation time. Table 2 demonstrates that the hydrogel copolymer solutions had gelation times of less than 7 s.

All the hydrogels displayed water content higher than 49% (Table 2). This was dependent on the AAc content and collagen addition. In general, hydrogels with higher amounts of AAc showed higher water content. Adding collagen into the hydrogel greatly increased the water content.

3.4. Hydrogel Mechanical Properties. Figure 4d and e show that the formed hydrogel was stretchable at 37 °C. Table 3 presents the hydrogel mechanical properties tested in a water bath at 37 °C. The hydrogels were highly extensible and soft with breaking strains greater than 1000% (exceeding the strain range of the mechanical tester), initial moduli from 39−119 KPa, and tensile stresses from 14.7−29.0 KPa. The tensile stress and modulus were related to the AAc content and collagen addition. An increase in AAc content was found to substantially

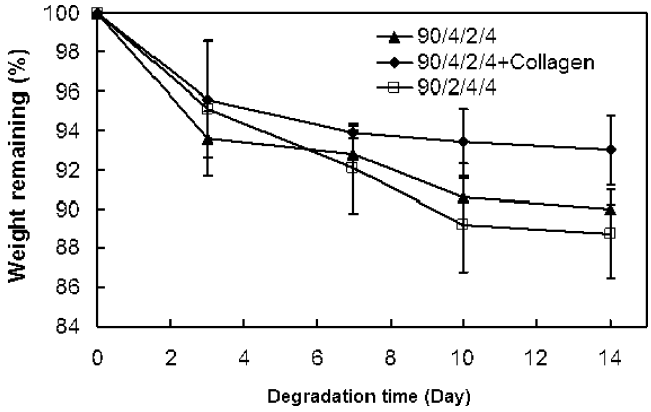

Figure 5. Degradation of hydrogels at 37 °C in PBS for 2 weeks. Hydrogel composition is listed in Table 1.

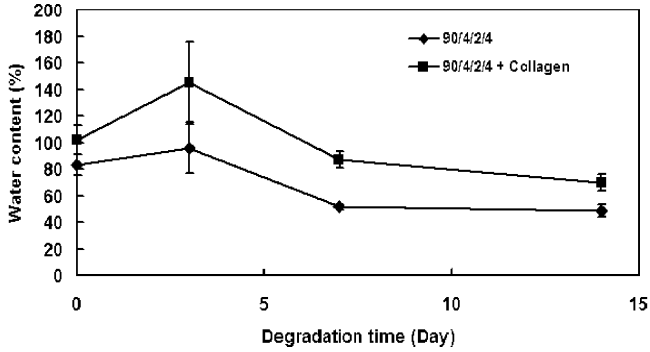

Figure 6. Water contents of hydrogels with and without collagen during the degradation.

Table 4. Superoxide Dismutase Encapsulation Efficiency

SOD concentration	collagen incorporation	encapsulation efficiency (%)
2 mg/mL	+	93
	−	89
4 mg/mL	+	95
	−	91

increase tensile stress and modulus. However, collagen addition significantly increased the tensile stress from 19.3−29.0 KPa ($p < 0.05$) and the modulus from 56.0−119.3 KPa ($p < 0.01$).

3.5. Hydrogel Degradation. Hydrogel degradation was conducted in PBS at 37 °C. All the hydrogels demonstrated progressive degradation during the 2 week period (Figure 5). By day 14, the hydrogels retained over 85% of their initial weight. When comparing the remaining weight of hydrogels 90/2/4/4 and 90/4/2/4, which had different AAc/DBA ratios, it was found that a change of AAc/DBA ratio from 1/2 to 2/1 did not alter the degradation rate. However, collagen incorporation significantly decreased the hydrogel degradation rate. Degradability of the hydrogel was further confirmed by GPC, where the number-average molecular weight of the completely degraded hydrogel (90/4/2/4) decreased from 13700 to 10100 Da.

Figure 6 shows the hydrogel water content change during degradation. Both hydrogel (90/2/4/4) and hydrogel biocomposite (90/2/4/4 + collagen) demonstrated a slight ($p > 0.05$) water content increase during the first 3 days, followed by a significant decrease at day 7 ($p < 0.01$ for both hydrogel and hydrogel biocomposite). However, extension of degradation time to day 14 did not significantly alter water content ($p > 0.05$ for both hydrogel and hydrogel composite).

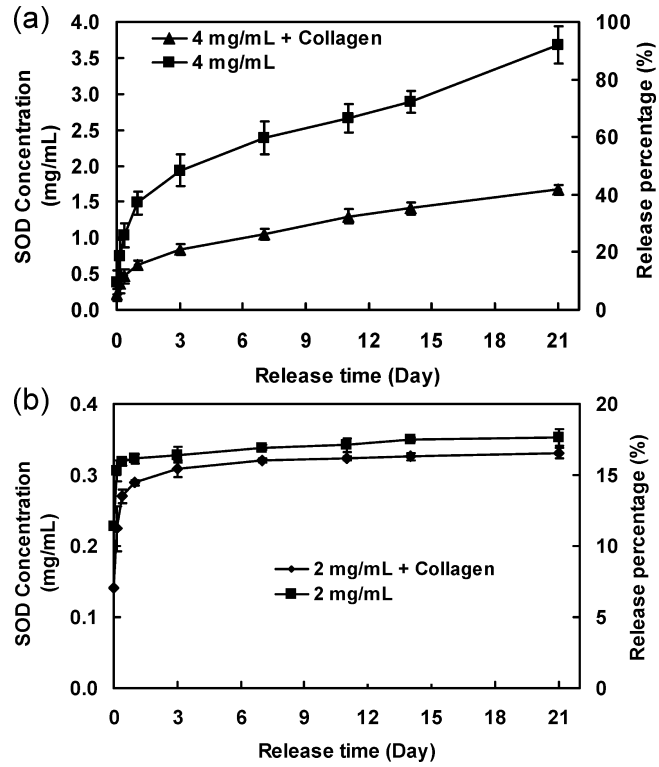

Figure 7. Release kinetics of SOD encapsulated in the hydrogels with or without collagen. SOD loading was 4 mg/mL (a) and 2 mg/mL (b), respectively.

3.6. SOD Release Kinetics and Bioactivity of Released SOD. Hydrogel copolymer 90/4/2/4 was selected for study of SOD delivery. SOD release was conducted in PBS at 37 °C for 3 weeks. The effect of collagen addition and SOD loading on release kinetics were investigated (Figure 7). Hydrogel/collagen biocomposite had a significantly slower release rate compared to hydrogel without collagen at each time point ($p < 0.05$), regardless of SOD loading. The hydrogel with lower SOD loading (2 mg/mL) demonstrated a two-stage release profile, a fast release during the first days, followed by a slow release from days 1−21. In contrast, the hydrogel with higher SOD loading (4 mg/mL) exhibited a more sustained release profile during the 3-week period. At each time point, the hydrogel with the higher SOD loading released a significantly higher amount of SOD than the hydrogel with the lower SOD loading (Table 4, $p < 0.05$).

Figure 8 shows that bioactivity of the released SOD is dependent on the SOD loading and collagen addition. For the hydrogel with the lower SOD loading (2 mg/mL), the released SOD preserved higher than 60% bioactivity for the first 2 weeks. This decreased to only above 40% in the third week. For the hydrogel with the higher SOD loading (4 mg/mL), the bioactivity of released SOD was consistently higher than 75% during the entire release period. SOD released from the hydrogel with or without collagen had similar bioactivity. As the mechanism for bioactivity assay used in this work was to quantitatively measure SOD bioactivity by its ability to inhibit superoxide generated by oxidation of xanthine in the presence of xanthine oxidase, these results indicated that SOD had a half-life of more than 2 weeks when encapsulated in the hydrogels.

3.7. MSC Culture in SOD-Loaded Hydrogel. To test the effect of SOD loading on cell proliferation, MSCs at a density of 10 million/mL were encapsulated within the hydrogels and hydrogel/collagen biocomposites with or without SOD. Cell growth was quantified by DNA content. Figure 9 shows that

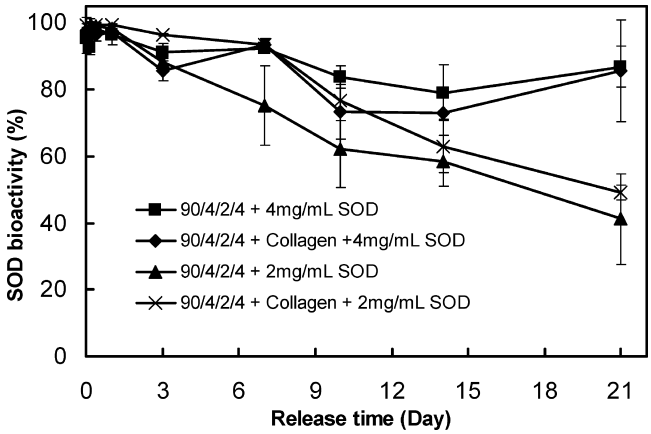

Figure 8. Bioactivity of released SOD from hydrogels with or without collagen and loaded with 4 or 2 mg/mL SOD.

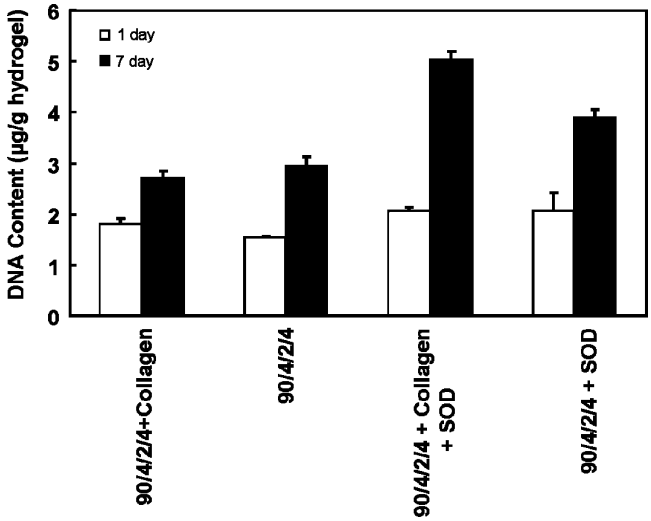

Figure 9. DNA content of MSCs encapsulated in the hydrogels with or without collagen and SOD (4 mg/mL) after 1 and 7 days of culture. DNA content was normalized with the weight of the hydrogel.

MSCs were capable of growing in all of the hydrogels with or without SOD loading during the 7 day culture period. At day 7, the SOD-loaded hydrogel and hydrogel/collagen biocomposite displayed significantly higher DNA content than those without SOD ($p < 0.05$), indicating that SOD loading reduced MSC apoptosis. For SOD-loaded hydrogels, collagen addition affected cell growth. The hydrogel/collagen biocomposite demonstrated a significantly greater DNA content than the hydrogel without collagen ($p < 0.05$).

Live cell staining in Figure 10 shows that MSCs in hydrogels remained alive during the 7 day culture period. For each hydrogel, the cell density was seen to increase during the culture. At day 7, the SOD-loaded hydrogel and hydrogel/collagen biocomposite had obviously higher cell density compared with their nonloaded counterparts.

3.8. Protection Effect of SOD on MSCs in the Presence of Superoxide. To investigate if SOD loading would protect MSCs from attack by superoxide, MSCs were labeled with a cell-permeant indicator (H_2DCFDA) that is nonfluorescent until the acetate groups are removed by intracellular esterases, and oxidation occurs within the cell. They were then encapsulated into the hydrogels. The cell encapsulated hydrogels were incubated in the medium containing superoxide generated by activated macrophages. After 4 and 20 h of incubation, the fluorescence intensities of SOD containing hydrogel with superoxide incubation, non-SOD containing hydrogel with superoxide incubation, and non-SOD containing hydrogel without superoxide incubation were measured and normalized to the hydrogel weight. The results showed that SOD containing hydrogel had a significantly lower fluorescence intensity than the non-SOD containing hydrogel at both 4 and 20 h (Figure 11). This demonstrates that SOD suppressed superoxide penetration into the hydrogel and thus the attack on MSCs as well.

4. Discussion

The main objective of this work was to develop injectable hydrogels that could be used as both stem cell and antioxidant carriers. Such a delivery system would not only be able to deliver stem cells but also create a protective microenvironment for stem cells from attack by reactive oxygen species (ROS) such as superoxide. In addition, the hydrogel provides a matrix for cell attachment to reduce apoptosis.[39] The hydrogels were synthesized by copolymerization of NIPAAm, AAc, DBA, and HEMAPTMC. The role of NIPAAm was to provide thermosensitivity. The AAC was used to increase solubility of the hydrogel. DBA was able to hydrolyze into AAc, which allowed the completely degraded polymer to have 6% of AAc and a thermal transition temperature >37 °C. Our previous work demonstrated that when AAc content was 6%, the degraded polymer would have a thermal transition temperature higher than 37 °C.[10] However, we found that if the hydrogel before degradation had 6% AAc, it had a fast dissolution rate in the buffer. Therefore, current hydrogels were designed with reduced initial AAc content. After hydrolysis of DBA, the formed AAc would allow the degraded polymers to have a total AAc content of 6%, allowing the polymer to be soluble at body temperature. HEMAPTMC was utilized to increase hydrophobicity of the hydrogel and decrease its thermal transition temperature to well below body temperature, so that gelation could occur at 37 °C before degradation. Table 2 and Figure 4 demonstrate that the hydrogels possessed thermal transition temperatures of around room temperature and were able to gel at 37 °C before degradation. After degradation, the hydrogel was soluble at 37 °C, as their thermal transition temperatures were well above 37 °C (Table 2).

Thermal transition temperatures of the hydrogels were dependent on AAc content (Table 2) and collagen addition. The hydrogel with higher AAc content demonstrated higher thermal transition temperatures. This is the result of an increase in hydrogel hydrophilicity, as the carboxylic acid group in the AAc unit is hydrophilic. The higher hydrophilicity would have greater inhibiting effect on the dehydration of the hydrogel polymer chain during the gelation process and, thus, result in higher thermal transition temperatures.[10] Likewise, adding hydrophilic collagen into the hydrogel increased the thermal transition temperature. Similarly, the water content was also affected by the hydrogel hydrophilicity, as hydrogel with higher AAc content or collagen addition demonstrated higher water content.

All hydrogel copolymer solutions were injectable at temperatures below thermal transition temperature (for example 4 °C) through a 26 gauge needle. This property is attractive as it would enable the hydrogels be easily delivered into tissues without causing substantial damage to the tissues.[40] In cell injection therapy, cells are usually delivered using needles as small as 26 gauge. This property also provides opportunities to deliver the hydrogels by minimally invasive surgery. The hydrogel copolymer solutions could form hydrogels at 37 °C within 7 s. This high gelation rate is expected to be beneficial for tissue

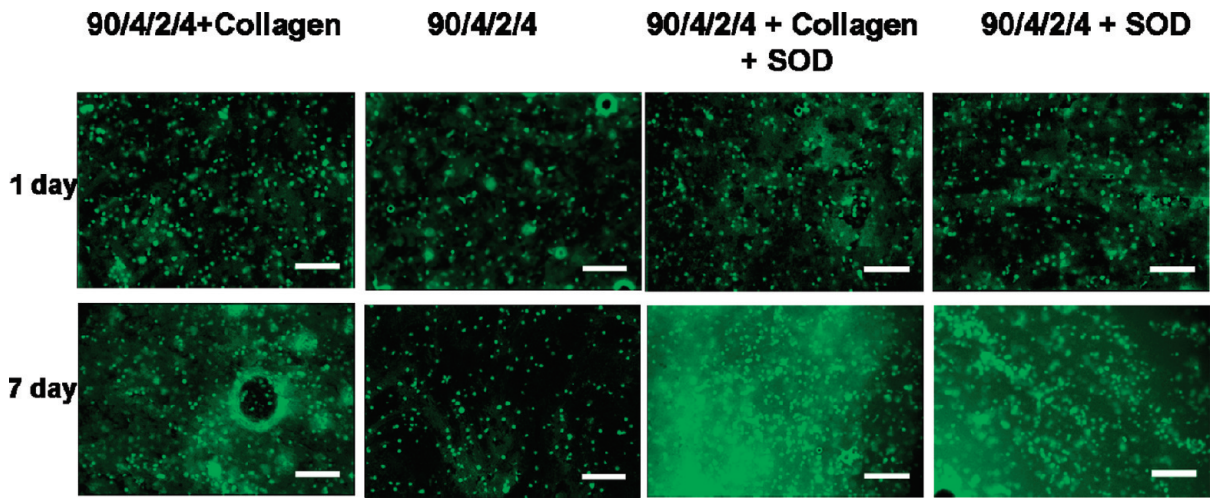

Figure 10. Fluorescence images of MSCs encapsulated in hydrogels with or without collagen and SOD (4 mg/mL) after 1 and 7 days of culture. The cells were stained with live cell stain CMFDA before encapsulation. Scale bar = 100 μm.

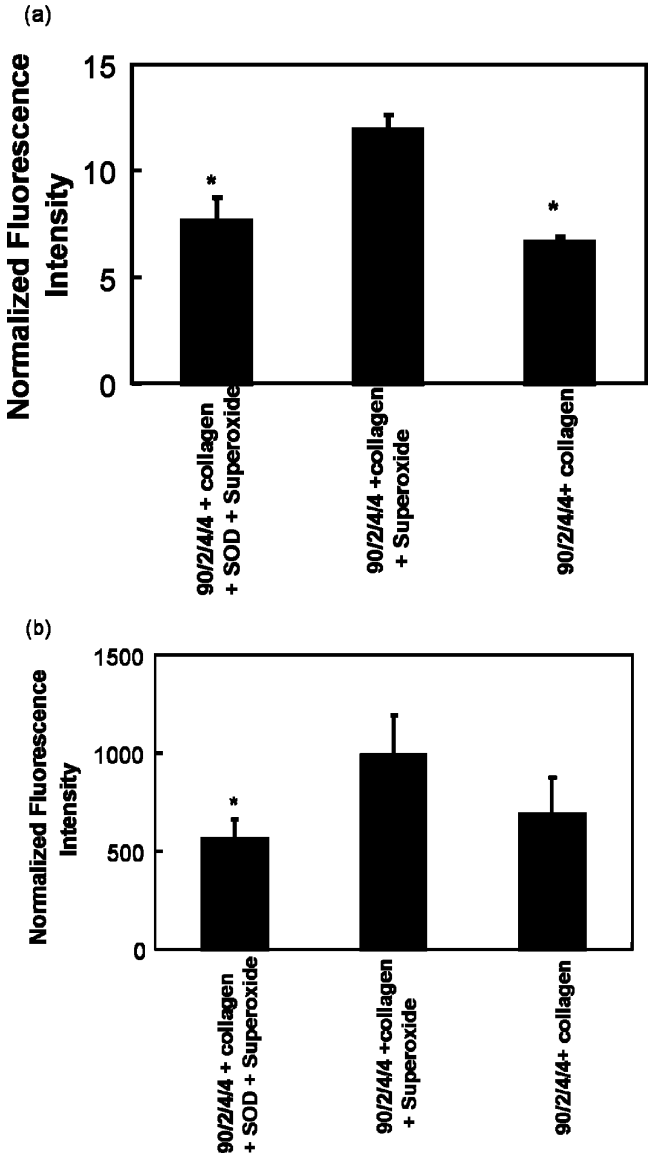

Figure 11. Fluorescence intensity of MSCs encapsulated hydrogels after culture in the medium with or without superoxide (generated by activated macrophage) for 4 h (a) and 20 h (b). MSCs were labeled with ROS sensitive dye H2DCFDA before being encapsulated into the hydrogel. SOD loading significantly inhibited superoxide penetration into the cell membrane. *$p < 0.05$.

injection, as the injected hydrogel could quickly solidify and localize within the tissue, thereby minimizing the possibility of the injected hydrogel leaking out. Furthermore, these fast gelling hydrogels could even be delivered into wounded tissues where a high density of capillaries and vasculatures are present, as it would decrease the possibility of the injected hydrogel blocking the blood flow and causing tissue necrosis. Indeed, this could occur for those slow gelling hydrogels.

All the hydrogels were highly flexible and soft with a breaking strain >1000% and with moduli ranging from 39 to 119 KPa (Table 3). The moduli of hydrogels were dependent on AAc content and collagen addition. Hydrogels with higher AAc content tended to have higher modulus. Collagen addition remarkably elevated the modulus from 56 to 119 KPa. This is possibly the result of an increased hydrogen bond interaction between carboxylic groups and amide bonds when AAc content increases and collagen is added. Hydrogel moduli were similar to those of rat and human myocardium (1−140 kPa for rat myocardium, and 20−500 kPa for human myocardium),[41] thus enabling them to be potentially used for myocardial cell therapy. The breaking strains and moduli are greater than those of collagen gel,[42] chitosan,[43] alginate,[44] and poly(ethylene glycol) (PEG)[45] hydrogels. These flexible hydrogels could be used for engineering mechano-active soft tissues possessing low moduli, as they would respond in concert with tissue motion and thus allow effective mechanical stimulus transfer from the tissue environment to the cells in the hydrogels during tissue regeneration. When placing stem cells and hydrogel into a tissue with similar modulus, the hydrogel may provide a native-like mechanical microenvironment for the stem cell to differentiate into appropriate cell types for enhanced tissue regeneration.[46] The importance of scaffold stiffness on stem cell growth and differentiation has been increasingly appreciated in recent years. It has been demonstrated that materials with different stiffness could direct stem cell to differentiate into different lineages.[44,47]

The hydrogels experienced progressive degradation during a 2 week period (Figure 5). At day 14, all the hydrogels retained over 85% of their initial weight. The change in AAc/DBA ratio from 1/2 to 2/1 did not significantly alter the degradation rate. However, collagen incorporation significantly decreased the degradation rate. It is possible that the electrostatic and hydrogen bond interactions between the collagen and carboxylic groups in the AAc unit delayed degraded water-soluble hydrogel from dissolving in the water. Interestingly, the hydrogel water content

decreased after 3 days of degradation. In the hydrogel, the longer polymer chains (higher molecular weight chains) aggregated to form a dense core, which was surrounded by a loose periphery region that consists of short polymer chains (lower molecular weight chains).[47] Water penetration into the loose periphery region is thus easier than into the dense core, leading to a higher water content and a faster degradation rate in the periphery region. Upon degradation of the periphery shorter polymer chains, the remaining dense core exhibits lower water content.

Current methods for SOD encapsulation are mainly focused on the use of microparticles and hydrogels. Microparticle delivery system consistently shows relatively low encapsulation efficiency (70−80%) and an inability to preserve long-term bioactivity (>1 week).[29−34] Studies using hydrogels as delivery vehicles displayed either a relatively short release time (<1 week) or low bioactivity of the released SOD.[52,53] Our hydrogel delivery system demonstrated much improved encapsulation efficiency (>89%) as well as the ability to preserve longer-term (3 weeks) bioactivity. SOD bioactivity is also much higher than that of the PEG-modified SOD, which only exhibited a half-life of 80 h.[29] SOD release kinetics and bioactivity were related to hydrogel degradation, water content, collagen addition, and SOD loading. During the first 3 days, degradation of smaller molecular weight macromolecules and relatively high water content enabled fast SOD release. This is evidenced by Figure 7, where all the hydrogels demonstrated burst release during the first 3 days. After 3 days, as both water content and degradation rate were decreased, all the hydrogels demonstrated slower release kinetics, indicating that SOD release may be dominated by both diffusion and hydrogel degradation. Incorporation of collagen did not significantly change bioactivity of the released SOD, though it slowed down the SOD release (Figure 7). This is due to the collagen addition decreased hydrogel degradation (Figure 5), which delayed SOD diffusion out of the hydrogel. The hydrogel with lower SOD loading demonstrated slower release kinetics compared with the hydrogel with higher SOD loading. This is possibly related to the interactions between SOD and hydrogel/collagen. At lower SOD loading (2 mg/mL), the SOD formed strong interactions with hydrogel/collagen, which restrained SOD release. At a higher SOD loading (4 mg/mL), not all of the SOD formed strong interactions with hydrogel/collagen. SOD that had weak interactions with hydrogel/collagen may have been released first.

MSCs were able to proliferate within the hydrogels during the 7 day culture period (Figures 9 and 10). Interestingly, SOD incorporation significantly stimulated MSC growth. It has been shown that ROS exists under the normal culture condition (37 °C, 20% O_2, and 5% CO_2), even in a medium containing antioxidant sodium pyruvate.[48,49] SOD loaded in the hydrogel may protect the cells from attack by ROS in the medium. This is consistent with recent studies that SOD could reduce apoptosis of MSCs transplanted in vivo.[24,30,50] Furthermore, we found that SOD in the hydrogel can efficiently protect encapsulated MSCs from attack by ROS when cultured in a medium containing superoxide generated by activated macrophages (Figure 11). After 4 and 20 h exposure to the superoxide, MSCs in the hydrogel containing SOD had significantly lower oxidative stress than those in the hydrogel without SOD, indicating that SOD significantly suppressed superoxide penetration into the hydrogel and cell membrane.

5. Conclusions

We synthesized novel injectable and thermosensitive copolymers based on *N*-isopropylacrylamide, acrylic acid, dimethyl-γ-butyrolactone acrylate, and macromer hydroxyethyl methacrylate-poly(trimethylene carbonate). The hydrogel copolymer solutions exhibited thermal transition temperatures of around room temperature with gelation able to occur within 7 s to form highly flexible and soft hydrogels. The degraded hydrogels were water-soluble at 37 °C. SOD was encapsulated in the hydrogels and demonstrated sustained release kinetics. The released SOD remained bioactive during the 3 week release period. The SOD-loaded hydrogels stimulated MSC growth and were confirmed to be capable of inhibiting superoxide attack on the cells. These hydrogels may have potential to be used as cell and drug carriers for cardiovascular applications.

Acknowledgment. We thank Dr. Jessica Winter for permitting use of fluorescence microscopy. This work was supported by Institute for Materials Research Facility Grant at the Ohio State University and in part by NIH RO1 HL073087.

Supporting Information Available. The validation of multipotency of human mesenchymal stem cell (passage 14) was conducted by RT-PCR (reverse transcriptase polymerase chain reactions). This material is available free of charge via the Internet at http://pubs.acs.org.

References and Notes

(1) Nicodemus, G. D.; Bryant, S. J. *Tissue Eng., Part B* **2008**, *14*, 149–165.
(2) Yow, S.; Quek, C.; Yim, E. K.; Lim, C.; Leong, K. *Biomaterials* **2009**, *30*, 1133–1142.
(3) Sawamura, K.; Ikeda, T.; Nagae, M.; Okamoto, S.; Mikami, Y.; Hase, H.; Ikoma, K.; Yamada, T.; Sakamoto, H.; Matsuda, K. I.; Tabata, Y.; Kawata, M.; Kubo, T. *Tissue Eng., Part A* **2009**, DOI: 10.1089/ten.tea.2008.0697.
(4) Chiu, Y.; Chen, S.; Su, C.; Hsiao, C.; Chen, Y.; Chen, H. *Biomaterials* **2009**, *30*, 4877–4888.
(5) Chung, C.; Beecham, M.; Mauck, R. L.; Burdick, J. A. *Biomaterials* **2009**, *30*, 4287–4296.
(6) Harada, A. *Coord. Chem. Rev.* **1996**, *148*, 115–133.
(7) Guo, M.; Jiang, M.; Pispas, S.; Yu, W.; Zhou, C. *Macromolecules* **2008**, *41*, 9744–9749.
(8) Benoit, D. S. W.; Schwartz, M. P.; Durney, A. R.; Anseth, K. S. *Nat. Mater.* **2008**, *7*, 816–823.
(9) Sanabria-DeLong, N.; Crosby, A. J.; Tew, G. N. *Biomacromolecules* **2008**, *9*, 2784–2791.
(10) Guan, J.; Hong, Y.; Ma, Z.; Wagner, W. R. *Biomacromolecules* **2008**, *9*, 1283–1292.
(11) Stile, R. A.; Burghardt, W. R.; Healy, K. E. *Macromolecules* **1999**, *32*, 7370–7379.
(12) Cui, Z.; Lee, B. H.; Vernon, B. L. *Biomacromolecules* **2007**, *8*, 1280–1286.
(13) Park, J. S.; Woo, D. G.; Yang, H. N.; Lim, H. J.; Park, K. M.; Na, K. *J. Biomed. Mater. Res., Part A* **2009**, DOI: 10.1002/jbm.a.32341.
(14) Sun, G.; Zhang, X.; Chu, C. *J. Mater. Sci.: Mater. Med.* **2008**, *19*, 2865–2872.
(15) Kim, S.; Chung, E. H.; Gilbert, M.; Healy, K. E. *J. Biomed. Mater. Res., Part A* **2005**, *75*, 73–88.
(16) Mias, C.; Lairez, O.; Trouche, E.; Roncalli, J.; Calise, D.; Seguelas, M. H.; Ordener, C.; Piercecchi-Marti, M.-D.; Negre Salvayre, A.; Bourin, P.; Parini, A.; Cussac, D. *Stem Cells* **2009**, DOI: 10.1002/stem.169.
(17) Huang, N. F.; Lam, A.; Fang, Q.; Sievers, R. E.; Li, S.; Lee, R. J. *Regener. Med.* **2009**, *4*, 527–538.
(18) Makino, S.; Fukuda, K.; Miyoshi, S.; Konishi, F.; Kodama, H.; Pan, J. *J. Clin. Invest.* **1999**, *103*, 697–705.
(19) Toma, C.; Pittenger, M. F.; Cahill, K. S.; Byrne, B. J.; Kessler, P. D. *Circulation* **2002**, *105*, 93–98.
(20) Shake, J. G.; Gruber, P. J.; Baumgartner, W. A.; Senechal, G.; Meyers, J.; Redmond, J. *Ann. Thorac. Surg.* **2002**, *73*, 1919–1926.
(21) Zhao, W.; Zhao, D.; Yan, R.; Sun, Y. *Cardiovasc. Pathol.* **2009**, *18*, 156–166.
(22) Andreadou, I.; Iliodromitis, E. K.; Farmakis, D.; Kremastinos, D. T. *Expert Opin. Ther. Targets* **2009**, *13*, 945–56.

(23) Inoue, T.; Ide, T.; Yamato, M.; Yoshida, M.; Tsutsumi, T.; Andou, M.; Utsumi, H.; Tsutsui, H.; Sunagawa, K. *Free Radic. Res.* **2009**, *43*, 37–46.
(24) Laurila, J. P.; Laatikainen, L. E.; Castellone, M. D.; Laukkanen, M. O. *PLoS One* **2009**, *4*, e5786.
(25) Greenlund, L. J. S.; Deckwerth, T. L.; Johnson, E. M. *Neuron* **1995**, *14*, 303–315.
(26) Cheung, C. Y.; McCartney, S. J.; Anseth, K. S. *Adv. Funct. Mater.* **2008**, *18*, 3119–3126.
(27) Axthelm, F.; Casse, O.; Koppenol, W. H.; Nauser, T.; Meier, W.; Palivan, C. G. *J. Phys. Chem. B* **2008**, *112*, 8211–8217.
(28) Chiumiento, A.; Domínguez, A.; Lamponi, S.; Villalonga, R.; Barbucci, R. *J. Mater. Sci.: Mater. Med.* **2006**, *17*, 427–435.
(29) Nakaoka, R.; Tabata, Y.; Yamaoka, T.; Ikada, Y. *J. Controlled Release* **1997**, *46*, 253–261.
(30) Abdel-Mageed, A. S.; Senagore, A. J.; Pietryga, D. W.; Connors, R. H.; Giambernardi, T. A.; Hay, R. V.; Deng, W. *Blood* **2009**, *113*, 1201–1203.
(31) Lee, S.; Yang, S. C.; Heffernan, M. J.; Taylor, W. R.; Murthy, N. *Bioconjugate Chem.* **2007**, *18*, 4–7.
(32) Çelik, Ö.; Akbuga, J. *Eur. J. Pharm. Biopharm.* **2007**, *66*, 42–47.
(33) Reddy, M. K.; Wu, L.; Kou, W.; Ghorpade, A.; Labhasetwar, V. *Appl. Biochem. Biotechnol.* **2008**, *151*, 565–577.
(34) Kaipel, M.; Wagner, A.; Wassermann, E.; Vorauer-Uhl, K.; Kellner, R.; Redl, H; Katinger, H.; Ullrich, R. *J. Aerosol Med. Pulm. Drug Delivery* **2008**, *21*, 281–290.
(35) Salvemini, D.; Riley, D. P.; Cuzzocrea, S. *Nat. Rev. Drug Discovery* **2002**, *1*, 367–374.
(36) Fujimoto, K. L.; Ma, Z.; Nelson, D. M.; Hashizume, R.; Guan, J.; Tobita, K.; Wagner, W. R. *Biomaterials* **2009**, *30*, 4357–4368.
(37) Song, L.; Tuan, R. S. *FASEB J.* **2004**, *18*, 980–982.
(38) Guan, J.; Stankus, J. J.; Wagner, W. R. *J. Controlled Release* **2007**, *120*, 70–78.
(39) Weber, L. M.; Hayda, K. N.; Haskins, K.; Anseth, K. S. *Biomaterials* **2007**, *28*, 3004–3011.
(40) Jeong, B.; Bae, Y. H.; Lee, D. S.; Kim, S. W. *Nature* **1997**, *388*, 860–862.
(41) Chen, Q. Z.; Harding, S. E.; Ali, N. N.; Lyon, A. R.; Boccaccini, A. R. *Mater. Sci. Eng., R* **2008**, *59*, 1–37.
(42) Elbjeirami, W. M.; Yonter, E. O.; Starcher, B. C.; West, J. L. *J. Biomed. Mater. Res., Part A* **2003**, *66*, 513–521.
(43) Tan, H.; Chu, C. R.; Payne, K. A.; Marra, K. G. *Biomaterials* **2009**, *30*, 2499–2506.
(44) Banerjee, A.; Arha, M.; Choudhary, S.; Ashton, R. S.; Bhatia, S. R.; Schaffer, D. V.; Kane, R. S. *Biomaterials* **2009**, *30*, 4695–4699.
(45) Bryant, S. J.; Arthur, J. A.; Anseth, K. S. *Acta Biomater.* **2005**, *1*, 243–252.
(46) Engler, A. J.; Carag-Krieger, C.; Johnson, C. P.; Raab, M.; Tang, H.; Speicher, D. W.; Sanger, J. W.; Discher, D. E. *J. Cell Sci.* **2008**, *121*, 3794–3802.
(47) Yim, H.; Kent, M. S.; Satija, S.; Mendez, S.; Balamurugan, S. S.; Balamurugan, S.; Lopez, G. P. *Phys. Rev. E* **2005**, *72*, 051801.
(48) Engler, A. J.; Sen, S.; Sweeney, H.; Discher, D. E. *Cell* **2006**, *126*, 677–689.
(49) Ramakrishnan, N.; Chen, R.; McClain, D. E.; Bünger, R. *Free Radic. Res.* **1998**, *29*, 283–295.
(50) Giandomenico, A. R.; Cerniglia, G. E.; Biaglow, J. E.; Stevens, C. W.; Koch, C. J. *Free Radic. Biol. Med.* **1997**, *23*, 426–434.
(51) Mias, C.; Trouche, E.; Seguelas, M. H.; Calcagno, F.; Dignat-George, F.; Sabatier, F.; Piercecchi-Marti, M. D.; Daniel, L.; Bianchi, P.; Calise, D.; Bourin, P.; Parini, A.; Cussac, D. *Stem Cells* **2008**, *26*, 1749–1757.
(52) Chiumiento, A.; Dominguez, A.; Lamponi, S.; Villalonga, R.; Barbucci, R. *J Mater Sci.: Mater Med.* **2006**, *17*, 427–435.
(53) Wang, B.; Zhu, W.; Zhang, Y.; Yang, Z. G.; Ding, J. D. *React. Funct. Polym.* **2006**, *66*, 509–518.

BM900900E